

Dysfunctional Prefrontal Cortical Network Activity and Interactions following Cannabinoid Receptor Activation

Michal T. Kucewicz,^{1,2} Mark D. Tricklebank,² Rafal Bogacz,³ and Matthew W. Jones^{1,2}

¹MRC Centre for Synaptic Plasticity, School of Physiology and Pharmacology, University of Bristol, BS8 1TD Bristol, United Kingdom, ²Centre for Cognitive Neuroscience, Eli Lilly and Co. Ltd., Windlesham, Surrey GU20 6PH United Kingdom, and ³Department of Computer Science, University of Bristol, BS8 1UB Bristol, United Kingdom

Coordinated activity spanning anatomically distributed neuronal networks underpins cognition and mediates limbic–cortical interactions during learning, memory, and decision-making. We used CP55940, a potent agonist of brain cannabinoid receptors known to disrupt coordinated activity in hippocampus, to investigate the roles of network oscillations during hippocampal and medial prefrontal cortical (mPFC) interactions in rats. During quiet wakefulness and rest, CP55940 dose-dependently reduced 0.1–30 Hz local field potential power in CA1 of the hippocampus while concurrently decreasing 30–100 Hz power in mPFC; these contrasting population-level effects were paralleled by differential effects on underlying single-unit activity in the two structures. During decision-making phases of a spatial working memory task, CP55940-induced deficits in hippocampal theta and prefrontal gamma oscillations were observed alongside disrupted theta-frequency coherence between the two structures. These changes in coordinated limbic–cortical network activities correlated with (1) reduced accuracy of task performance, (2) impaired phase-locking of prefrontal single-unit spiking to the local gamma and hippocampal theta rhythms, and (3) impaired task-dependent activity in a subset of mPFC units. In addition to highlighting the importance of CA1–mPFC network oscillations for cognition, these results implicate disrupted theta-frequency coordination of CA1–mPFC activity in the cognitive deficits caused by exogenous activation of brain cannabinoid receptors.

Introduction

Information processing in the brain is distributed across anatomically segregated neuronal networks and therefore necessitates large-scale integration of parallel network computations. Both local processing and transfer of information between distinct brain regions are facilitated by temporal organization of network activities (Gray, 1994; von Stein and Sarnthein, 2000; Varela et al., 2001; Fries, 2005; Fell and Axmacher, 2011), which manifests as local field potential (LFP) and EEG oscillations spanning a range of frequency bands. One important example is the 5–10 Hz theta rhythm known to organize the timing of principal cell firing in the hippocampus (O'Keefe and Recce, 1993), resulting in preferential spiking on consistent phases of the ongoing theta cycle. Behavior-dependent phase alignment to hippocampal theta also occurs in amygdala (Pape et al., 2005), dorsal and ventral striatum (Tort et al., 2008; van der Meer and Redish, 2011), and prefrontal cortex (Siapas et al., 2005), prompting the concept of a theta phase code transmitted via coordinated oscillations be-

tween hippocampus and functionally connected brain regions (Hasselmo, 2005; Jensen and Lisman, 2005). Hippocampal–prefrontal interactions in the theta frequency range have been consistently implicated in functions associated with working memory in rats and humans (Jones and Wilson, 2005; Anderson et al., 2010; Benchenane et al., 2010; Hyman et al., 2010) and provide a potential mechanism for integration of mnemonic and decision-making processes during goal-directed behaviors (Sauseng et al., 2010; Fell and Axmacher, 2011). Accordingly, aberrant oscillatory activity is associated with impaired cognition in a wide range of neuropsychiatric disorders (Uhlhaas and Singer, 2006) and may cause and/or reflect impaired limbic–cortical interactions in disease.

Δ^9 -THC, the primary psychoactive ingredient of cannabis, exerts its psychotropic effects by activating brain cannabinoid receptors, which are prominently expressed in structures associated with cognition, including hippocampus, neocortex, basal ganglia, and cerebellum (Herkenham et al., 1990; Glass et al., 1997). Cannabinoid receptor agonists are known to reduce the power of network oscillations in the hippocampus and neocortex (Buonamici et al., 1982; Morrison et al., 2011), and recently, Robbe and colleagues showed that disrupted theta coordination of principal cell firing in the rat hippocampus correlated with spatial working memory impairments induced by systemic cannabinoid receptor agonists (Robbe et al., 2006; Robbe and Buzsáki, 2009). They concluded that proper theta timescale coordination of neuronal spiking in the hippocampus is critical for spatial working memory, even though spatial information content of place cell firing was not affected. Here, we used the

Received June 13, 2011; revised Sept. 1, 2011; accepted Sept. 9, 2011.

Author contributions: M.D.T. and M.W.J. designed research; M.T.K. performed research; M.T.K., R.B., and M.W.J. analyzed data; M.T.K., M.D.T., and M.W.J. wrote the paper.

This work was supported by a Medical Research Council Industrial Collaborative Studentship award to M.D.T. and M.W.J. We thank Tom Jahans-Price for providing the Maze Query Language toolbox used for the analysis of rat trajectories and unit firing on the maze, and Debi Ford for expert assistance with histology.

The authors declare no financial conflicts of interest.

Correspondence should be addressed to Dr. Matthew W. Jones, School of Physiology and Pharmacology, University of Bristol, University Walk, BS8 1TD Bristol, United Kingdom. E-mail: matt.jones@bristol.ac.uk.

DOI:10.1523/JNEUROSCI.2970-11.2011

Copyright © 2011 the authors 0270-6474/11/3115560-09\$15.00/0

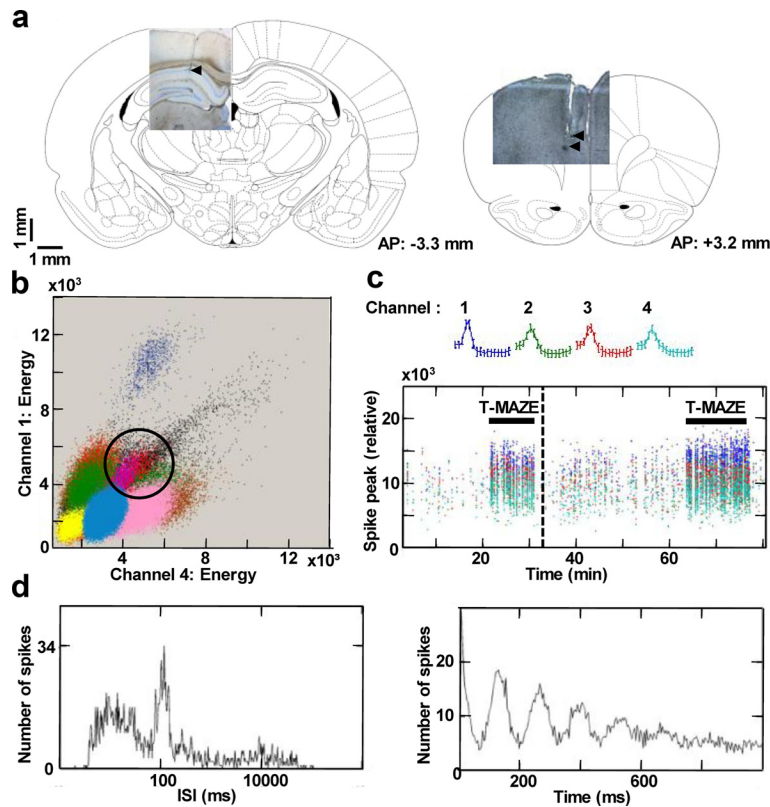


Figure 1. Extracellular tetrode recordings of single-unit activity. **a**, Representative micrographs of Giemsa-stained 50 μm brain slices showing the sites of *post hoc* electrolytic lesions (arrowheads) in the principal cell layer of the dorsal CA1 (left) and prelimbic subdivision of the medial prefrontal cortex (right) fitted to a schematic of corresponding rat brain section (from rat brain atlas by Paxinos and Watson, 1998). **b**, Thirteen color-coded clusters of action potentials spread along the axes of relative energy recorded on two channels of a tetrode in CA1. The properties of the red cluster (circled) are shown in **c** and **d**. **c**, Mean waveform recorded on color-coded channels of the tetrode (top) showing stable relative spike amplitudes throughout one T-maze experiment (bottom). Note the behavioral modulation of firing rate during the first (predrug) and the second (postdrug) T-maze epochs (horizontal black bars). Dashed vertical line marks the time of drug administration. **d**, Distribution of interspike intervals (ISI) and autocorrelation for all spikes fired by the unit in the experimental session. Notice the characteristic hippocampal theta modulation of unit firing (~ 100 ms interspike intervals).

potent cannabinoid receptor agonist CP55940 to investigate whether cannabinoid signaling impacts coordinated network oscillations beyond the hippocampus. In particular, since functional disconnection of the CA1 and mPFC impairs spatial working memory in rats (Floresco et al., 1997; Wang and Cai, 2006), we hypothesized that pharmacological disruption of the temporal coordination between hippocampal and prefrontal cortical networks would impair the information exchange necessary to guide spatial memory-based decisions.

Materials and Methods

In vivo electrophysiological recordings. All procedures were conducted in accordance with the UK Animals (Scientific Procedures) Act, 1986 and with the approval of the University of Bristol Ethics Committee. Six adult (300–400 g) male Long–Evans rats (Harlan) were chronically implanted with 20 extracellular tetrode recording electrodes: 10 into deep layers of the right prelimbic cortex (+3.2 mm, +0.6 mm from bregma) and 10 into CA1 in the right dorsal hippocampus (−3.6 mm, +2.2 mm from bregma) under sodium pentobarbital recovery anesthesia. During the 7–12 d following surgery, the independently moveable tetrodes were lowered into the brain, targeting the prelimbic subdivision of the prefrontal cortex (~ 2 –3 mm ventral) and pyramidal cell layer in the dorsal CA1 (verified by the characteristic burst mode of single-unit firing and the presence of large-amplitude sharp-wave ripple events in the LFP signal). Recordings were made using a Digital Lynx system (Neuralynx). Local field potentials (sampled at 2 kHz and filtered between 0.1–475 Hz) and extracellular action potentials (sampled at 30 kHz and filtered between 0.6–6 kHz) were recorded differentially using local references,

which were left in the superficial prefrontal cortex and in the white matter overlying the hippocampus. All channels were grounded to two screws placed in the skull overlying the cerebellum. Final tetrode tip positions were verified histologically by identifying sites of electrolytic lesions (see Fig. 1a) made at the end of experimental procedures under terminal anesthesia. Only one LFP channel from hippocampus and one from prefrontal cortex of each rat were chosen for subsequent analyses based on the amplitude of ripple events and the coherence to hippocampal theta oscillations, respectively.

Recording protocols. Data were recorded in a rest box and during an end-to-end T-maze task. Three doses (0.03, 0.15, 0.30 mgkg^{-1} intraperitoneal) of CP55940 (Tocris Bioscience) or vehicle solution (10% ethanol, 10% cremophor, 80% saline) were used. In rest box experiments, each subject was placed on a padded plate (20 cm diameter) inside a wooden box (45 \times 45 \times 100 cm). Animal movement was confined by the size of the plate and monitored continuously by video. Injections were administered at least 20 min into the experiment and data were recorded for another 60 min. Analyses were performed at 10 min intervals preinjection and postinjection (at least 10 min into the experiment and 30 min after injection, respectively), based on the time courses of behavioral (Lichtman et al., 1995; Wise et al., 2009) and network activity (Robbe et al., 2006; Hajós et al., 2008; Robbe and Buzsáki, 2009) changes exerted by systemic injections of cannabinoid receptor agonists in rats. Five of the subjects were subsequently trained in an end-to-end T-maze spatial working memory task (for a description, see Jones and Wilson, 2005) after being food-restricted to 85% of free feeding body weight. Beginning from a guided reward location, rats were required to run along the central

arm of the maze and choose between left or right turns at the T-junction toward reward points; the correct choice was contingent on the side of the previously visited sample location. Rats were then guided by moveable barriers back to a sample location G, with trial-by-trial location pseudorandomly assigned (no more than three consecutive trials on the same side). Both the guided and the choice runs were reinforced with a sugar pellet on the correct trials; no reinforcement was provided on the incorrect trials. Location of the guided and choice ends of the maze in the recording room was varied between animals. Experimental sessions comprised a predrug block of trials, followed 30 min later by postdrug task performance. Subjects had to complete 14–25 trials in each stage and only 5 s intervals of choice run epochs (from 3.5 s before the decision point to 1.5 s after) were analyzed. Position during task performance was video tracked using light-emitting diodes attached to a powered headstage (Cheetah software; Neuralynx).

Data analysis. All data were processed in Matlab (Mathworks) unless stated otherwise. Multitaper Fourier analyses (Chronux toolbox; Bokil et al., 2010) were used to calculate power and coherence of the LFP data. For statistical comparison, four bands of the LFP oscillations were used, as follows: 0.1–4 Hz (delta), 5–10 Hz (theta), 30–60 Hz (low gamma), and 60–100 Hz (high gamma). Single units were isolated off-line (Fig. 1b,c) using automated clustering software (Kluster 1.7; K. Harris, available at <http://klustakwik.sourceforge.net/>), followed by verification and manual refinement using MClust 3.5 (A. D. Redish, available at <http://redishlab.neuroscience.umn.edu/MClust/MClust.html>); inclusion criteria were set to isolation distance >15.0 and L-ratio <0.35 . Putative pyramidal cells were classified on the basis of the spike width, waveform,

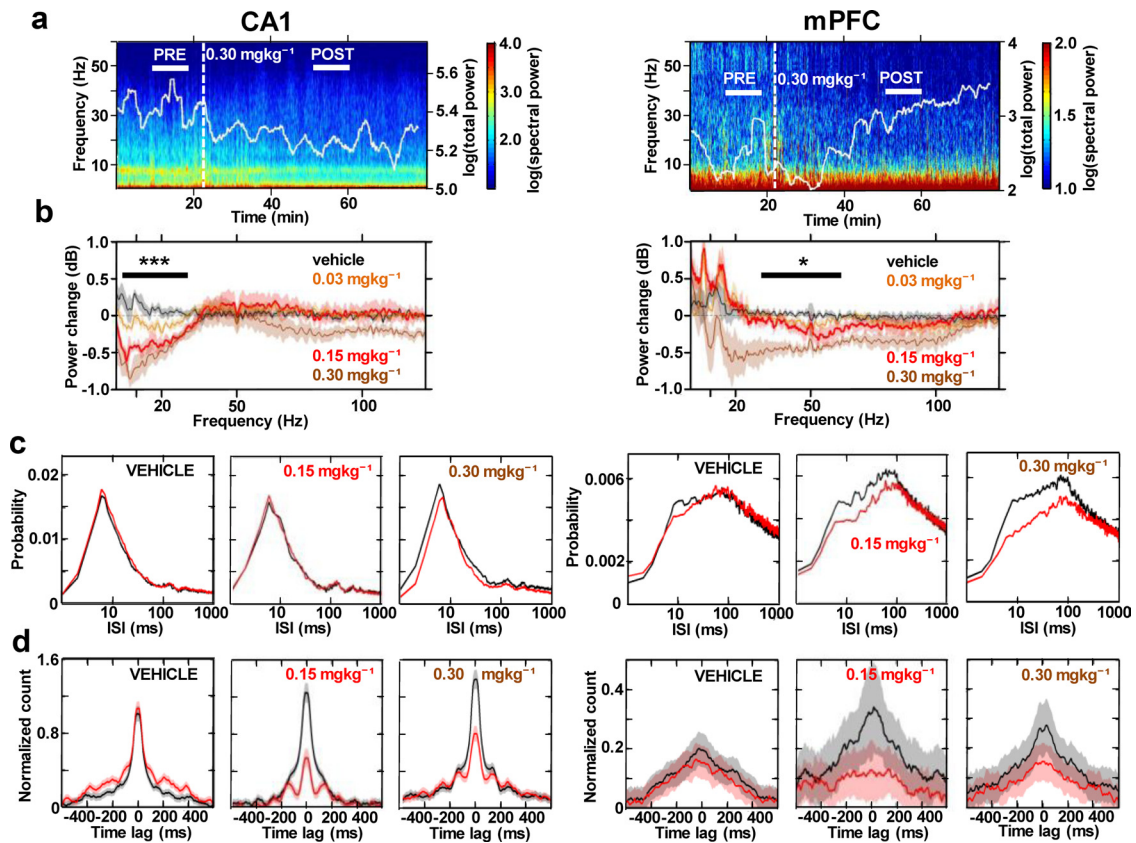


Figure 2. Cannabinoid receptor activation causes differential changes in network oscillations and single-unit activity in CA1 and mPFC. Data from simultaneous CA1 and mPFC recordings are presented on the left and right, respectively. *a*, Power spectrograms (1 Hz bandwidth, 5 s sliding time window with 2 s overlap) of local field potential oscillations (2–60 Hz range) throughout the course of one rest box experiment. White trace signifies the total power changes of the broadband LFP signal (0.1–475 Hz). Dashed vertical line marks the time of drug injection. Horizontal white bars indicate the preinjection (PRE) and postinjection (POST) intervals used for subsequent analyses of drug effects on LFP power and single-unit activity. *b*, Subject-averaged ($N = 6$) change in LFP power across a 125 Hz range of oscillations at three doses of CP55940 and its vehicle. Horizontal bars mark frequency ranges over which CP55940 caused significant, dose-dependent decreases in power (tested by repeated-measures ANOVA). Note the differential effects of the intermediate dose highlighted in dark red. *c*, Interspike interval (ISI) distributions comparing predrug and postdrug (black and red lines, respectively) single-unit activity following vehicle ($n = 68$ and 73 putative pyramidal cells in CA1 and mPFC respectively), 0.15 mg kg⁻¹ ($n = 62$ and 59) or 0.30 mg kg⁻¹ ($n = 73$ and 53) of CP55940. *d*, Cross-correlogram plots (10 ms bins) of all possible cell pair combinations accompanied by analogous plots from the vehicle control experiment, as in *c*. * $p < 0.05$, *** $p < 0.001$.

and mean firing rate. Autocorrelograms were computed in Neuroexplorer (Nex Technologies), including only the units that fired a minimum of 50 spikes in the preinjection and postinjection periods. Cross-correlograms were computed in Matlab and shuffle-corrected using spike trains shifted by ± 1 s to cancel out effects of nonstationarities in the firing rate due to state transitions (e.g., non-REM to REM sleep), then normalized by their asymptotic mean firing rates (Robbe et al., 2006). Butterworth bandpass filters were used to filter LFP for the phase-locking analyses. Circular statistics quantifying spike phase distribution (Siapas et al., 2005) of every classified unit were calculated to estimate the mean population phase-locking or to determine significantly phase-locked units at $p < 0.05$. When comparing effects of CP55940 on phase-locking, the numbers of predrug and postdrug spikes were matched by randomly selecting a subset of spikes from whichever epoch contained fewer events.

Local field potential power changes in the rest box experiment and the central arm position tracking data were compared using repeated-measures ANOVA. LFP power and coherence changes and behavioral performance were evaluated with nonparametric Wilcoxon signed rank test. Single-unit data were analyzed by comparing matched preinjection and postinjection parameters for every single unit using two-tailed paired t test. Maze trajectories were selected using Maze Query Language toolbox (T. Jahans-Price and R. Bogacz, available at <http://www.cs.bris.ac.uk/Research/MachineLearning/mql/>). Statistical significance was assessed in SPSS Statistical Package (SPSS). Data are presented as mean \pm SEM.

Results

Network oscillations and single-unit activity during quiet wakefulness

We first examined the effects of systemic, intraperitoneal CP55940 administration on network oscillations and the associated activity of isolated single units in dorsal CA1 of the hippocampus and prelimbic subdivision of the medial prefrontal cortex (mPFC) in rats (Fig. 1) at rest on a 20 cm diameter platform. Rats were judged to be predominantly in a state of quiet wakefulness based on video recording and LFP signal on-line monitoring. In agreement with previous studies using Δ^9 -THC (Buonamici et al., 1982; Robbe et al., 2006), CP55940 primarily decreased the power of theta rhythm in CA1, as evidenced by fading of spectral power in the 5–10 Hz band 20–60 min following drug injection (Fig. 2*a*, left). In contrast, the mPFC spectrogram did not reveal directly comparable alterations in this lower frequency range of network oscillations (Fig. 2*A*, right). Dose-dependent reductions in 0.1–30 Hz low-frequency power in CA1 (repeated-measures ANOVA, $F_{(3,15)} = 20.8$, $p < 0.001$, $N = 6$; Fig. 1*b*, left) were contrasted by significant decreases in 30–100 Hz gamma power in mPFC (repeated-measures ANOVA, $F_{(3,15)} = 7.81$, $p = 0.02$; Fig. 2*b*,

right). Thus, CP55940 differentially modulated network oscillations in the two structures.

To elucidate the cellular correlates of these differential effects on network oscillations, we examined the firing properties of putative pyramidal cells in the two structures following 0.30 mg/kg doses of CP55940. This dose of the drug decreased firing rates of putative pyramidal cells in CA1 ($p = 0.017$, $n = 73$) but not in mPFC ($p = 0.57$, $n = 53$; data not shown); 0.15 mg/kg doses had no significant effects on firing rates in the two networks (CA1: $p = 0.35$, $n = 64$; mPFC: $p = 0.72$, $n = 41$). Interspike interval distributions revealed only a slight decrease in CA1 unit burst firing in the 4–10 ms interspike interval range induced by the drug ($p = 0.082$, $n = 73$; Fig. 2c, left), contrasted by a significant reduction in burst firing in mPFC ($p = 0.016$, $n = 53$ cells), which also extended across the 10–100 ms range ($p = 0.048$; Fig. 2c, right). This may contribute to the observed decrease in the power of prefrontal gamma oscillations in mPFC, given that spiking with 10–30 ms interspike intervals may accompany 30–100 Hz gamma rhythms in network oscillations. Similarly, the slight decrease in burst firing in CA1 units could account for the small reduction in the high-frequency LFP oscillations (>100 Hz) observed at 0.30 mg/kg dose of the drug (Fig. 2b, left).

The lack of any major alterations in hippocampal autocorrelograms, despite a profound decline in low-frequency power, suggests that the firing patterns of individual units may be less essential than coordination across populations in generating lower-frequency oscillations. This corroborates previous suggestions that the reduced power of hippocampal network oscillations following cannabinoid receptor activation may stem from decreased coordination of spiking between neurons (Katona et al., 1999; Robbe et al., 2006). In agreement with this hypothesis, cross-correlation analysis of all possible pairs of units revealed markedly decreased probabilities of synchronous firing of CA1 units in a ± 100 ms window (paired t test, $p < 0.001$, $n = 1038$ cell pairs; Fig. 2d, left), as previously reported (Robbe et al., 2006). This effect was also significant at the 0.15 mg/kg dose (paired t test, $p < 0.001$, $n = 956$ cell pairs; Fig. 2d, left). mPFC units also showed a decreased peak of cross-correlated activity following drug administration (Fig. 2d, right), but this effect was not as pronounced as in CA1. Overall, these results are consistent with the idea that coordinated activity across populations of cells is important for maintaining network oscillations in the lower part of the LFP frequency spectrum (0.1–30 Hz), as shown in the CA1 network activity, whereas the rhythmic firing of individual neurons appears to be critical for sustained oscillations at the higher frequencies (30–200 Hz), such as gamma in the prefrontal cortex.

Network oscillations during a spatial working memory task

We used a spatial working memory paradigm based on an end-to-end T-maze (Jones and Wilson, 2005) to assess the functional relevance of the network activity changes induced by CP55940 (see Materials and Methods, above; Fig. 3a). In rodents, agonists of CB1 receptors are known to have detrimental effects on spatial working memory (Lichtman et al., 1995; Wise et al., 2009) and here we report a severe impairment (Wilcoxon signed rank test, $p = 0.007$, $N = 5$; Fig. 3b) in task choice accuracy, which dropped to chance level following administration of the intermediate dose (0.15 mg/kg) of the drug. This was the minimal dose that impaired rats on this task without inducing gross behavioral abnormalities and was therefore used for all subsequent analyses. At 0.15 mg/kg, CP55940 had a small but significant effect on running speed, increasing time taken to cross the central arm run of

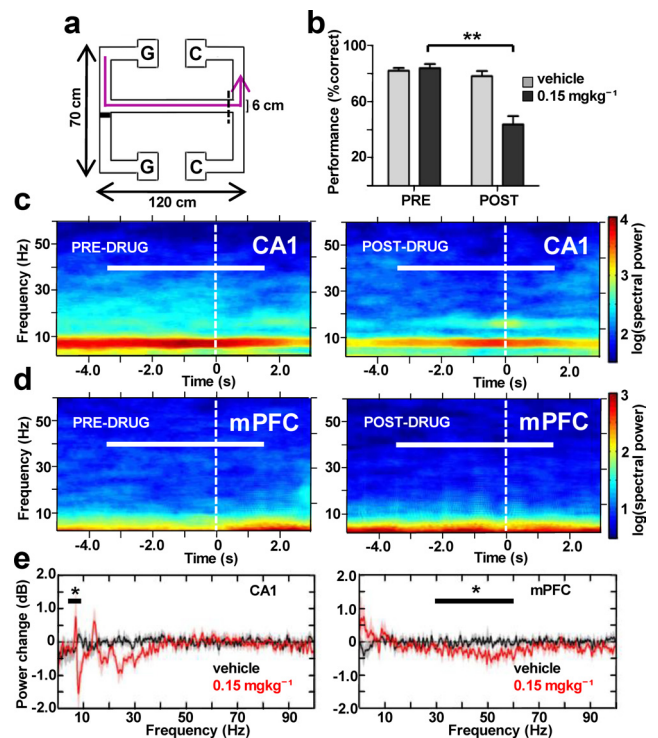


Figure 3. Hippocampal and prefrontal cortical LFP power changes in the spatial working memory task. **a**, Schematic diagram of the double-ended T-maze showing the path trajectory of one trial (magenta line) beginning in the guided-turn reward point (G), followed by central arm run with a turn decision point (dashed line) and ending in choice turn reward location (C) (see Materials and Methods). **b**, Accuracy of task performance before and after administration of the drug (0.15 mg/kg) or its vehicle ($N = 5$). $^{***}p < 0.01$. **c, d**, Spectrograms (2 Hz bandwidth, 1 s sliding time window with 0.01 s overlap) of LFP power changes in CA1 (**c**) and mPFC (**d**) on approach to the decision point (white dashed line) during trial-averaged choice runs ($n = 17$ and 15 trials) in one representative experiment before and after administration of 0.15 mg/kg of the drug. Horizontal white bars indicate the time interval used for all subsequent analyses. **e**, Subject-averaged ($N = 5$) change in LFP power (1 Hz bandwidth, 1 s time window) across the 100 Hz range of oscillations at one dose of CP55940 used (0.15 mg/kg) and its vehicle. Horizontal bars span the theta and gamma frequency bands over which mean power was compared. $^{*}p < 0.05$.

the maze (1.11 s predrug, 1.65 s postdrug, $p = 0.039$). However, the overall durations of incorrect trial runs were not significantly different from the correct runs in the nondrug condition ($p = 0.85$), suggesting that working memory failures were not solely due to increased latency to reach the decision point.

We focused our analyses on the choice run periods of the task preceding and immediately following the decision point on the T-maze, when cognitive load is at its highest and CA1–mPFC theta frequency interactions are at their peak (Fig. 3a) (Jones and Wilson, 2005; Benchenane et al., 2010; Hyman et al., 2010). Elevated hippocampal theta power evident throughout these choice runs was attenuated postdrug ($p = 0.041$; Fig. 3c), an effect previously attributed to direct actions of the drug plus reduced running speed (Robbe and Buzsáki, 2009). Compared with the results of the rest box power analysis (Fig. 2), this suppression of hippocampal LFP power was confined to the theta (5–10 Hz) band during running. In mPFC, there was a significant reduction in the power of low gamma (30–60 Hz) oscillations under these conditions ($p = 0.043$; Fig. 3e, right). Additionally, there was a trend for increased delta (0.1–4 Hz) power in mPFC and a significant decrease in the beta (22–30 Hz) band power in CA1 ($p = 0.043$; Fig. 3e, left).

Disrupted hippocampal–prefrontal LFP coherence

As rats approach the decision point at the choice T-junction, the LFP signal in mPFC becomes coherent with CA1 oscillations in the theta range; theta coherence is significantly greater during correct choice than during incorrect choice or guided runs (Jones and Wilson, 2005) and peaks following task rule acquisition (Benchenane et al., 2010). This dynamic coordination of CA1–mPFC activity is thought to signify information exchange required for successful spatial working memory performance, and coincides with increased spatial information content in the firing of mPFC units (Jones and Wilson, 2005). Corroborating these previous findings, we observed a consistent hotspot of elevated theta coherence immediately preceding the decision point during pre-drug choice runs (Fig. 4*a*, left); this coherence transient was severely attenuated postdrug (Fig. 4*a*, right). Averaging over subjects, the distinct peak in theta frequency coherence was centered on a frequency slightly <8 Hz, and fell below the 95% confidence level as a result of drug administration (Fig. 4*b*): mean values of coherence calculated in the 7–9 Hz peak band were significantly decreased post-CP55940 ($p = 0.021$), but were unaffected by control vehicle injections (Fig. 4*c*). Pooling all maze experiments using all three doses of the drug (0.03–0.30 mg/kg) revealed a positive correlation between the 7–9 Hz coherence and the accuracy of task performance when calculated either for all datasets (Pearson correlation, $r = 0.729$, $p < 0.01$; Fig. 4*d*, black line) or just for 0.15–0.30 mg/kg data points (Pearson correlation, $r = 0.793$, $p = 0.019$; Fig. 4*d*, dashed line). We therefore provide further evidence for the importance of theta range communication between CA1 and mPFC networks in spatial working memory functions.

As shown in previous work (Jones and Wilson, 2005), although CA1 and mPFC LFP power spectra during runs toward both the guided and choice turns were similar, theta coherence during guided runs was not significant. It is therefore not possible to assess whether cannabinoid receptor activation disrupted coordination at times of low cognitive load, though CA1 and mPFC LFP power was attenuated during guided runs. Nevertheless, it is possible that cannabinoid signaling is selectively recruited during alignment of CA1–mPFC activity, hence CP55940-induced impairments manifest preferentially during task phases that recruit CA1–mPFC interactions.

Selective and state-dependent disruption of theta-frequency phase locking

The population-level alignment of CA1 and mPFC reflected by LFP theta-frequency coherence is paralleled at the cellular level by phase-locking of spike times to both local and remote LFP oscillations (Fig. 5*a*). To quantify the degree of phase-locking and its modulation by CP5540, mean values of the circular concentration coefficient were determined for CA1 and mPFC units (Jones and Wilson, 2005). Though drug-induced changes in single-unit firing rates were not detected in either structure (paired t test: CA1, $p = 0.12$; mPFC, $p = 0.81$) during epochs of central arm choice runs, the number of spikes in the predrug and postdrug condition was matched to eliminate the effect of unequal spike numbers on phase-locking. Mean population

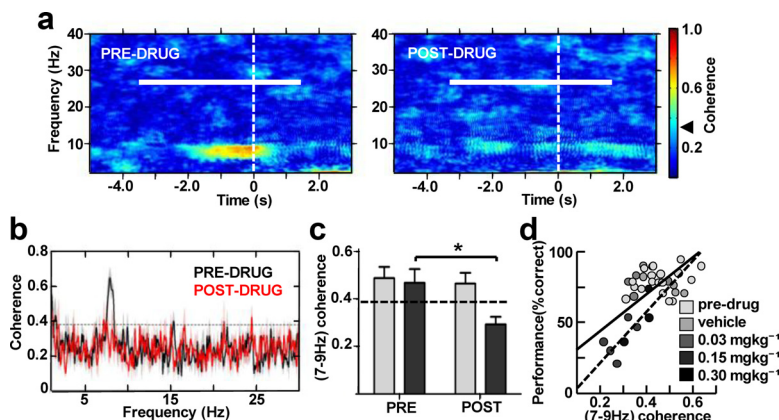


Figure 4. Disruption of hippocampal–prefrontal LFP coherence in the theta range correlates with behavioral impairment in the spatial working memory task. *a*, Coherograms (2 Hz bandwidth, 1 s sliding window with 0.1 s overlap) illustrating the effects of CP55940 (0.15 mg/kg) on LFP coherence between CA1 and mPFC during runs toward the decision point (dashed line) from the same experiment corresponding to power spectrograms in Figure 3. Horizontal white bars indicate the time interval of choice run used for all subsequent analyses. Black arrowhead on the color scale points to 95% confidence level of coherence. *b*, Hippocampal–prefrontal LFP coherence (1 Hz bandwidth) over 2–30 Hz frequency range averaged over subjects ($N = 5$) following 0.15 mg/kg CP55940. Confidence level at $p = 0.05$ is delineated by black dashed line. *c*, Averaged 7–9 Hz coherence ($N = 5$) comparing drug effect in the vehicle (light gray) and 0.15 mg/kg (dark gray) experiments. *d*, Scatter plot of performance accuracy and corresponding mean hippocampal–prefrontal 7–9 Hz coherence from all 36 maze sessions. Black lines (continuous for all dataset; dashed for 0.15 mg/kg and 0.30 mg/kg data points) show Pearson's correlation analysis signifying positive correlation at the 0.01 level. * $p < 0.05$.

circular concentration values were proportional to the number of units showing significantly nonuniform circular spike distribution ($p < 0.05$, Rayleigh test of nonuniformity).

We first examined the population phase-locking of single units in CA1 ($n = 41$) and mPFC ($n = 47$) to three bands of local network LFP oscillations (theta: 5–10 Hz; low gamma: 30–60 Hz; high gamma: 60–100 Hz) during central arm choice runs. Despite the large decreases in the power of the theta rhythm, population phase-locking to theta within CA1 (Fig. 5*b*, left) was not significantly altered by 0.15 mg/kg CP55940 ($p = 0.067$). No intra-CA1 changes were detected in the other LFP bands. In mPFC, there was a significant decrease in locking to low gamma oscillations ($p = 0.006$; Fig. 5*b*, right), with 19% of units (9/47) exhibiting significant phase-locking predrug and no significantly locked units postdrug; this is in accord with the reduced LFP power in this band during maze choice runs (Fig. 3). There was no change in mPFC local theta phase-locking.

To assess CA1–mPFC network interactions, we conducted the same analysis for prefrontal unit phase-locking ($n = 53$) to CA1 theta oscillations, first during the preinjection and postinjection intervals of the rest box experiment (Fig. 5*c*, left). The drug (0.30 mg/kg) had no effect in these resting state conditions, with 13/53 (25%) and 11/53 (21%) PFC units showing significant CA1 theta phase-locking predrug and postdrug, respectively. However, the same analysis conducted for the T-maze epochs of the central arm choice runs revealed a profound deficit in mPFC unit phase-locking to CA1 theta rhythm (paired t test, $p = 0.006$, $n = 47$; Fig. 5*c*, right) following CP5540 (0.15 mg/kg): 36% of mPFC units (17/47) were significantly phase-locked to the CA1 theta rhythm in this condition, dropping to 15% (7/47) following the drug. There was no significant change in phase-locking to the other LFP bands and the general degree of population phase-locking was elevated relative to the rest box conditions, implying that the effects of the cannabinoid receptor agonist on CA1–mPFC interactions are specific to the theta frequency band and

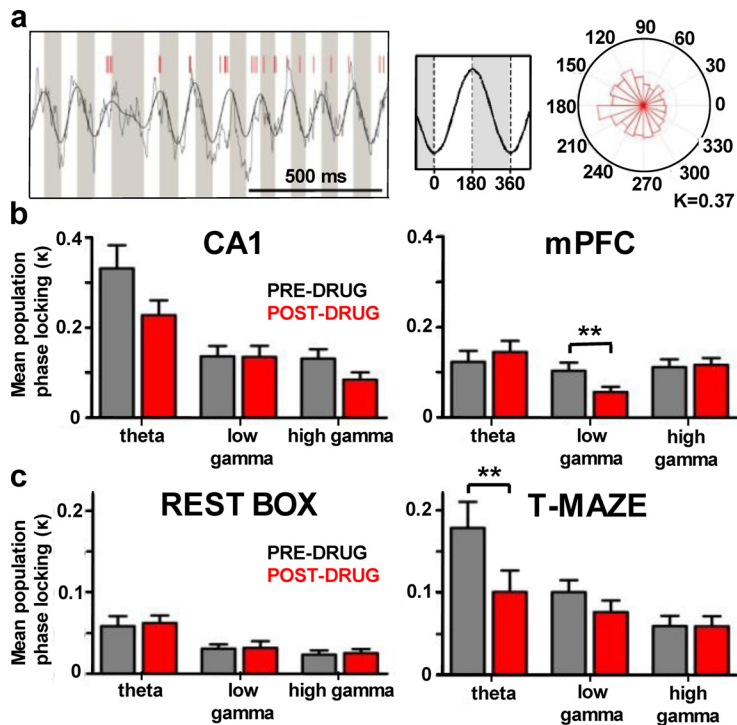


Figure 5. Single units display state-dependent deficits in phase-locking to specific bands of LFP oscillations. *a*, An example of one hippocampal unit showing preferential spiking (red tick marks) on distinct phases of the concurrent LFP oscillation (bandpass filtered for at 5–10 Hz) during a single choice central arm crossing. Rose diagram shows the distribution of spikes fired by the unit around the phases of the theta cycle. Theta phase-locking is quantified by circular-concentration coefficient (K). *b*, Mean population phase-locking of hippocampal and prefrontal single units ($n = 41$ and 47 cells) to three bands of their network LFP oscillations during preinjection and postinjection (0.15 mgkg^{-1}) choice runs. *c*, Analogous bar plots showing mean population phase-locking of prefrontal units to hippocampal local field oscillations during preinjection and postinjection intervals (0.30 mgkg^{-1}) of the rest box experiment ($n = 53$ cells) and during preinjection and postinjection session (0.15 mgkg^{-1}) choice runs of the T-maze experiment ($n = 47$ cells). Note that the drug has a profound effect on the theta unit phase-locking only in the working memory condition, even though higher dose was used in the rest box condition. $**p < 0.01$.

more pronounced when animals are actively engaged in a cognitive task.

Behavioral impairment and turn-selective neurons

To further investigate the consequences of disrupted limbic–cortical theta communication for animal behavior, we analyzed the left- and right-turn running trajectories. Rats revealed clearly distinct trajectories of correct left and right choice runs, measured as the effect of longitudinal central arm segments (repeated-measures ANOVA, $F_{(8,64)} = 8.970$, $p < 0.001$, $N = 5$) and segments \times turn interaction ($F_{(8,64)} = 6.613$, $p < 0.001$) on the central arm position of rats approaching the decision point (Fig. 6*a*, bottom left). Rats showed significant bias toward the pending correct turn direction, particularly in the last three segments of the central arm (0.30 m ; $F_{(1,8)} = 6.132$, $p = 0.038$), presumably reflecting the decision-making process biasing rats toward the correct destination. During predrug and postdrug error trials, there was still a significant effect of segment ($F_{(8,64)} = 4.775$, $p < 0.001$ and $F_{(8,64)} = 4.464$, $p < 0.001$ respectively), but the segment \times turn interaction was no longer significant, and was much weaker for the drug condition ($F_{(8,64)} = 1.295$, $p = 0.262$ and $F_{(8,64)} = 0.223$, $p < 0.985$, respectively; Fig. 6*a*, bottom). Rats therefore lose prospective bias toward the correct turn direction during both predrug and postdrug errors, as measured by between-subject factor of turn for the last three segments of the central arm ($F_{(1,8)} = 1.077$, $p = 0.330$ and $F_{(1,8)} = 0.080$, $p = 0.784$, respectively).

Running trajectory-selective neuronal activity might reflect any bias signal guiding subjects toward the correct location. We therefore looked for units that displayed turn-selective activity, i.e., exhibited differential firing on the correct left and right choice trials during the last three positional bins of the central arm (Fig. 6*b*). Firing rates of all units were calculated for each bin and compared between left and right choice runs to determine turn-selectivity ($p < 0.05$, t test). Figure 6*c* illustrates a typical example of an mPFC turn-selective neuron alongside corresponding running trajectories (Fig. 6*b*). The neuron shows low firing rates in the initial bins of the central arm, which increase as the rat approaches the decision point and are significantly higher for the left versus right choice runs even before the turn is made (Fig. 6*c*, left). Thirty minutes following 0.15 mgkg^{-1} CP55940, the same neuron still shows the build-up of activity toward the decision but no longer exhibits discriminative firing between left and right turns (Fig. 6*c*, right). This loss of turn-selective firing cannot be explained solely by more overlapping postdrug running trajectories in the central arm, since the neuron still fails to discriminate between the two turns in the drug condition even in the last arm segment, when the trajectories have already diverged to the left and right arms of the T-junction (Fig. 6*b*, *c*).

Seven of 47 mPFC neurons analyzed (15%) were found to be turn-selective (Fig. 6*d*) before drug administration; this fraction is higher than the 5% expected by chance (assuming a random variable with binomial distribution with $p = 0.05$). Five of these lost their turn-selectivity after drug administration. Turn-selective units in the hippocampus made up 7% of the population recorded ($3/41$) and their proportion was not affected by the drug (Fig. 6*D*). Loss of turn-selective firing in the prefrontal cortex is one plausible consequence of the disrupted theta-range communication, preventing the processing of spatial information across hippocampal and the prefrontal cortical networks.

Discussion

We show that impairments in a spatial working memory task caused by systemic activation of cannabinoid receptors in rats were accompanied by disrupted temporal coordination of neuronal activity both within and across hippocampal and prefrontal cortical networks. In addition to distinct changes in local field potential oscillations of dorsal CA1 and mPFC, there was a concurrent disruption of theta range interactions between the two networks, which manifested as reduced theta coherence and decreased phase-locking of mPFC units to the CA1 theta rhythm during memory-based decisions in the T-maze. These effects on network oscillations and interactions are likely to contribute to the cognitive deficits elicited by exogenous agonists of brain cannabinoid receptors.

Delay-dependent impairments in spatial memory tasks induced by cannabinoid receptor agonists have so far been attrib-

uted to mechanisms confined to the hippocampus and mediated by the CB₁ receptors (Lichtman et al., 1995; Wise et al., 2009). These receptors are predominantly expressed on basket-type interneurons expressing cholecystokinin (CCK); together with parvalbumin-containing interneurons, CCK interneurons form the basis of a neuronal network able to clock oscillations by providing windows of opportunity for synchronized discharge of pyramidal cells between phasic release of GABA (Klausberger et al., 2005). Cannabinoids therefore presumably desynchronize rhythmic network coordination in CA1 by activating CB₁ receptors on CCK-positive interneurons and decreasing the release of GABA (Katona et al., 2000; Hajós et al., 2008). Much less is known about the effect of exogenous cannabinoids in other structures; evidence for cellular distribution of the CB₁ receptors in the neocortex is limited and controversial, implicating other groups of interneurons and pyramidal neurons alongside CCK-positive basket cells (Bodor et al., 2005; Hill et al., 2007). The differential effects of the cannabinoid receptor agonist on LFP oscillations and single-unit activity in mPFC that we present here may therefore result from various differences in the network architecture, cannabinoid receptor expression, and/or endocannabinoid signaling machinery relative to CA1.

CP55940-induced changes in prefrontal cortical network activity included decreases in LFP gamma power and reduced phase-locking of mPFC units to lower gamma (30–60 Hz) oscillations during the delay period preceding the decision point on the maze. Gamma frequency oscillations have been implicated in human working memory (Howard et al., 2003) and a similar phenomenon of unit phase-locking to lower gamma oscillations has recently been reported to occur in monkey prefrontal cortex in a visual short-term memory task (Siegel et al., 2009), hence these changes may contribute to behavioral effects of systemic CB₁ receptor activation; they also potentially implicate CCK-positive interneurons in mediating or modulating cortical gamma rhythms.

In rats, both hippocampus and prefrontal cortex appear to be required for working memory tasks, albeit through processing of different informational components (Yoon et al., 2008); while dorsal hippocampus is adapted to encode and process spatial information, prelimbic cortex coordinates signaling about current spatial goals (Hok et al., 2005). In essence, the exchange of information between these two structures seems to be necessary when spatial memory guides goal-directed behavior, as suggested by the hippocampal–prefrontal cortical disconnection studies (Floresco et al., 1997; Wang and Cai, 2006). In rat, the two networks are anatomically and physiologically connected (Laroche et al., 2000) and dynamically coupled by means of theta range interactions (Jones and Wilson, 2005; Benchenane et al., 2010; Hyman et al., 2010). Here, we have shown that disruption of this theta band communication between CA1 and mPFC correlates with impairment in working memory performance. We suggest that

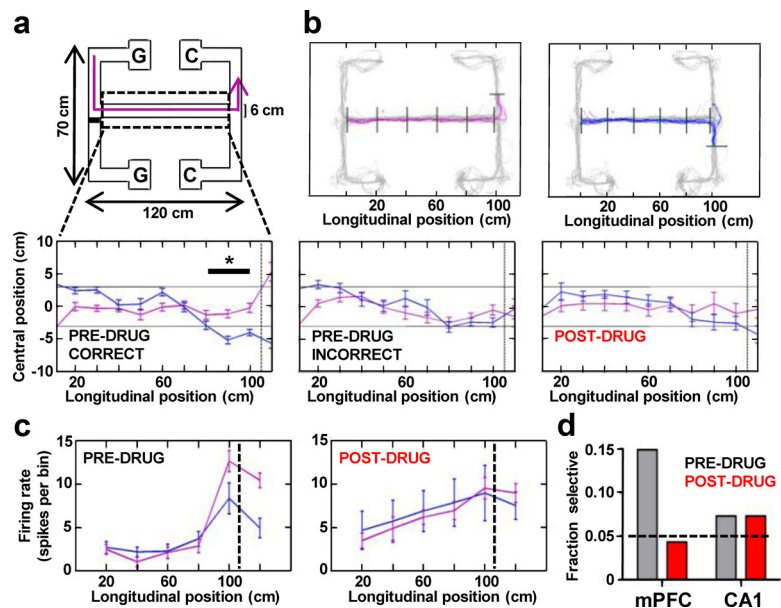


Figure 6. CP55940-induced behavioral impairment in the spatial working memory task is accompanied by loss of turn-selective firing in prefrontal cortex. *a*, Schematic diagram of one correct left-turn trial run (magenta line) from the sample location (G) to the goal choice location (C). Below, Enlarged top views of subject-averaged ($N = 5$) central arm trajectories from correct predrug, incorrect predrug, and postdrug runs toward the decision point marked by vertical dashed line. Magenta and blue indicate left and right choice runs, respectively. The black bar indicates the last three segments of the central arm preceding the decision point. Note that the two trajectories are significantly separated in these last three segments for the correct trials, but overlap for incorrect and postdrug conditions. *b*, Tracking data from one experiment showing left (magenta) and right (blue) choice predrug runs with position bins (divided by black lines) over which firing rates of single units were calculated. *c*, Firing rate of an example prefrontal turn-selective neuron during the corresponding choice runs shown in *c*. Note that the unit shows increased selective firing just before the decision point (dashed line), which is lost following the drug. *d*, Bar plot shows total fraction of all cells ($n = 47$ and 41 cells) showing turn-selective firing in CA1 and mPFC before and after the drug (0.15 mg kg^{-1}). Dashed line signifies the expected 0.05 chance occurrence of turn-selective units. $*p < 0.05$.

this disruption of hippocampal–prefrontal information processing culminates in the loss of prefrontal unit turn-selective firing and is directly related to the CP55940-induced impairment in the task. To our knowledge, this is the first demonstration of state-dependent pharmacological disruption of functional connectivity between limbic–cortical networks involved in execution of working memory-dependent processes.

Although theta rhythmic coordination between prefrontal and medial temporal lobe structures has been implicated in human working memory processes (Raghavachari et al., 2001; Anderson et al., 2010; Sauseng et al., 2010), the exact functions and mechanism of these processes are current topics of investigation and debate. CP55940-induced impairments in spatial working memory could be ascribed to a combination of highly interdependent processes of sustained attention, working memory, and decision-making. Furthermore, theta-frequency alignment may facilitate information flow top-down from neocortical networks to the hippocampus to support retrieval and maintenance of spatial memory and/or bottom-up, to supply prefrontal cortex with encoded spatial information to guide goal-directed behavior. Previous work suggests that the latter is the case, with CA1 leading mPFC (Siapas et al., 2005); disruption of turn-selective neurons following reduced CA1–mPFC coherence in our experiments would support this hypothesis, but paradigms using different task strategies and manipulations will be required to determine the exact role of the theta range interactions and their dependence on cannabinoid signaling.

One possibility is that the CA1–mPFC system acts as a working memory buffer dependent on activity at theta and gamma

frequencies (Hasselmo, 2005; Jensen and Lisman, 2005). In this view, individual items are encoded and sequentially indexed along the phase of the theta wave into episodic representations and transferred between hippocampus and functionally coupled neocortical sites as a theta phase code (Lisman and Buzsáki, 2008). Such theta-coordinated activity has been reported in the medial prefrontal cortex (Jones and Wilson, 2005) and the ventral striatum (van der Meer and Redish, 2011) in rats. Activation of brain cannabinoid receptors was shown to disrupt the theta phase code in the hippocampus in a manner that correlated with accuracy of performance in a spatial alternation task (Robbe and Buzsáki, 2009). Here we show evidence for a collateral deficit in theta phase-locking in the medial prefrontal cortex and we conjecture that the theta phase code transferred to the prefrontal cortex is essential to understanding cannabinoid-induced working memory deficits. Disruption of the theta phase code provides an intuitive neural mechanism for cannabinoid-induced cognitive impairment that Melges et al. (1970) called “temporal disintegration” and described as “difficulty in retaining, coordinating and serially indexing those memories, perceptions and expectations that are relevant to the goal one is pursuing.”

Links between cognitive impairments and aberrant network oscillations are increasingly implicated in the pathophysiology of schizophrenia (Uhlhaas and Singer, 2010; Haenschel and Linden, 2011), and alterations in rhythmic activity in the theta, alpha, beta, and gamma bands of cortical oscillations have been reported to correlate with working memory dysfunction in the disease (Haenschel et al., 2009; Haenschel and Linden, 2011). Moreover, disrupted functional coupling between dorsolateral prefrontal cortex and hippocampus has been observed in schizophrenia patients (Lawrie et al., 2002; Meyer-Lindenberg et al., 2005) as well as in healthy carriers of a genetic risk variant (Eslinger et al., 2009) and a mouse model of a chromosomal microdeletion associated with the disease (Sigurdsson et al., 2010). Altogether, the profile of acute changes in hippocampal and prefrontal cortical network oscillations and interactions following systemic CP5540 closely overlaps with changes implicated in cognitive symptoms of schizophrenia. Given the parallels between cognitive symptoms and cognitive impairments following cannabinoid activation—particularly in the domains of working and episodic memory (Fletcher and Honey, 2006; Solowij and Michie, 2007)—it seems likely that cannabinoid signaling contributes to the dynamic coordination of limbic–cortical interactions central to mnemonic processing, and that systemic CB₁ receptor activation presents a useful model of cognitive impairment related directly to limbic–cortical dysfunction.

The validity of acute pharmacological models with respect to schizophrenia's chronic time course in general, and causative or compensatory reduction of expression of postmortem, prefrontal CB₁ receptor expression in particular (Eggen et al., 2008), remains to be established. Furthermore, intravenous Δ^9 -THC administration in healthy volunteers can induce positive (psychotic) symptoms of schizophrenia potentially linked to aberrant intracortical network coordination (Koethe et al., 2009; Morrison et al., 2011) and cannabinoid dysfunction may therefore relate to, and be used to model, broader aspects of the disease, not just cognitive dysfunction. NMDA receptor antagonists are also noted for their psychotomimetic properties, and induce cognitive impairments and distinct changes in neuronal oscillations reminiscent of schizophrenia (Fletcher and Honey, 2006; Lazarewicz et al., 2010; Gilmour et al., 2011). These commonalities between CB₁ receptor activation and NMDA receptor blockade potentially reflect convergence of glutamatergic and cannabinoid-

nergic systems at the level of interneuronal networks (Puighermanal et al., 2009). Hence, both NMDA receptor antagonists and cannabinoid receptor agonists offer useful pharmacological tools for modeling key aspects of cognitive disorders. In combination with the use of network oscillations as biomarkers of altered cognition (Uhlhaas and Singer, 2006), these tools will continue to shed light on the neural mechanisms of working memory and decision making in health and disease.

Notes

Supplemental material for this article is available at <http://www.bristol.ac.uk/phys-pharm/media/pubs/jones/kucewiczetal-jn-supplinfo.pdf>. Classification of putative pyramidal cells based on spike width. This material has not been peer reviewed.

References

- Anderson KL, Rajagovindan R, Ghacibeh GA, Meador KJ, Ding M (2010) Theta oscillations mediate interaction between prefrontal cortex and medial temporal lobe in human memory. *Cereb Cortex* 20:1604–1612.
- Benchenane K, Peyrache A, Khamassi M, Tierney PL, Gioanni Y, Battaglia FP, Wiener SI (2010) Coherent theta oscillations and reorganization of spike timing in the hippocampal-prefrontal network upon learning. *Neuron* 66:921–936.
- Bodor AL, Katona I, Nyíri G, Mackie K, Ledent C, Hájós N, Freund TF (2005) Endocannabinoid signaling in rat somatosensory cortex: laminar differences and involvement of specific interneuron types. *J Neurosci* 25:6845–6856.
- Bokil H, Andrews P, Kulkarni JE, Mehta S, Mitra PP (2010) Chronux: a platform for analyzing neural signals. *J Neurosci Methods* 192:146–151.
- Buonamici M, Young GA, Khazan N (1982) Effects of acute delta-9-THC administration on EEG and EEG power spectra in the rat. *Neuropharmacology* 21:825–829.
- Eggen SM, Hashimoto T, Lewis DA (2008) Reduced cortical cannabinoid 1 receptor messenger RNA and protein expression in schizophrenia. *Arch Gen Psychiatry* 65:772–784.
- Eslinger C, Walter H, Kirsch P, Erk S, Schnell K, Arnold C, Haddad L, Mier D, Opitz von Boberfeld C, Raab K, Witt SH, Rietschel M, Cichon S, Meyer-Lindenberg A (2009) Neural mechanisms of a genome-wide supported psychosis variant. *Science* 324:605–.
- Fell J, Axmacher N (2011) The role of phase synchronization in memory processes. *Nat Rev Neurosci* 12:105–118.
- Fletcher PC, Honey GD (2006) Schizophrenia, ketamine and cannabis: evidence of overlapping memory deficits. *Trends Cogn Sci* 10:167–174.
- Floresco SB, Seamans JK, Phillips AG (1997) Selective roles for hippocampal, prefrontal cortical, and ventral striatal circuits in radial-arm maze tasks with or without a delay. *J Neurosci* 17:1880–1890.
- Fries P (2005) A mechanism for cognitive dynamics: neuronal communication through neuronal coherence. *Trends Cogn Sci* 9:474–480.
- Gilmour G, Dix S, Fellini L, Gastambide F, Plath N, Steckler T, Talpos J, Tricklebank M (2011) NMDA receptors, cognition and schizophrenia—testing the validity of the NMDA receptor hypofunction hypothesis. *Neuropharmacology*. Advance online publication. doi:10.1016/j.neuropharm.2011.03.015.
- Glass M, Dragunow M, Faull RL (1997) Cannabinoid receptors in the human brain: a detailed anatomical and quantitative autoradiographic study in the fetal, neonatal and adult human brain. *Neuroscience* 77:299–318.
- Gray CM (1994) Synchronous oscillations in neuronal systems: mechanisms and functions. *J Comput Neurosci* 1:11–38.
- Haenschel C, Linden D (2011) Exploring intermediate phenotypes with EEG: working memory dysfunction in schizophrenia. *Behav Brain Res* 216:481–495.
- Haenschel C, Bittner RA, Waltz J, Haertling F, Wibrall M, Singer W, Linden DE, Rodriguez E (2009) Cortical oscillatory activity is critical for working memory as revealed by deficits in early-onset schizophrenia. *J Neurosci* 29:9481–9489.
- Hájós M, Hoffmann WE, Kocsis B (2008) Activation of cannabinoid-1 receptors disrupts sensory gating and neuronal oscillation: relevance to schizophrenia. *Biol Psychiatry* 63:1075–1083.
- Hasselmo ME (2005) What is the function of hippocampal theta rhythm? Linking behavioral data to phasic properties of field potential and unit recording data. *Hippocampus* 15:936–949.
- Herkenham M, Lynn AB, Little MD, Johnson MR, Melvin LS, de Costa BR,

- Rice KC (1990) Cannabinoid receptor localization in brain. *Proc Natl Acad Sci U S A* 87:1932–1936.
- Hill EL, Gallopin T, Férézou I, Cauli B, Rossier J, Schweitzer P, Lambollez B (2007) Functional CB1 receptors are broadly expressed in neocortical GABAergic and glutamatergic neurons. *J Neurophysiol* 97:2580–2589.
- Hok V, Save E, Lenck-Santini PP, Poucet B (2005) Coding for spatial goals in the prelimbic/infralimbic area of the rat frontal cortex. *Proc Natl Acad Sci U S A* 102:4602–4607.
- Howard MW, Rizzuto DS, Caplan JB, Madsen JR, Lisman J, Aschenbrenner-Scheibe R, Schulze-Bonhage A, Kahana MJ (2003) Gamma oscillations correlate with working memory load in humans. *Cereb Cortex* 13:1369–1374.
- Hyman JM, Zilli EA, Paley AM, Hasselmo ME (2010) Working memory performance correlates with prefrontal-hippocampal theta interactions but not with prefrontal neuron firing rates. *Front Integr Neurosci* 4:2.
- Jensen O, Lisman JE (2005) Hippocampal sequence-encoding driven by a cortical multi-item working memory buffer. *Trends Neurosci* 28:67–72.
- Jones MW, Wilson MA (2005) Theta rhythms coordinate hippocampal-prefrontal interactions in a spatial memory task. *PLoS Biol* 3:e402.
- Katona I, Sperlágth B, Sik A, Käfalvi A, Vizi ES, Mackie K, Freund TF (1999) Presynaptically located CB1 cannabinoid receptors regulate GABA release from axon terminals of specific hippocampal interneurons. *J Neurosci* 19:4544–4558.
- Katona I, Sperlágth B, Maglóczy Z, Sántha E, Köfalvi A, Czirkák S, Mackie K, Vizi ES, Freund TF (2000) GABAergic interneurons are the targets of cannabinoid actions in the human hippocampus. *Neuroscience* 100:797–804.
- Klausberger T, Marton LF, O'Neill J, Huck JH, Dalezios Y, Fuentealba P, Suen WY, Papp E, Kaneko T, Watanabe M, Csicsvari J, Somogyi P (2005) Complementary roles of cholecystokinin- and parvalbumin-expressing GABAergic neurons in hippocampal network oscillations. *J Neurosci* 25:9782–9793.
- Koethe D, Hoyer C, Leweke FM (2009) The endocannabinoid system as a target for modelling psychosis. *Psychopharmacology* 206:551–561.
- Laroche S, Davis S, Jay TM (2000) Plasticity at hippocampal to prefrontal cortex synapses: dual roles in working memory and consolidation. *Hippocampus* 10:438–446.
- Lawrie SM, Buechel C, Whalley HC, Frith CD, Friston KJ, Johnstone EC (2002) Reduced frontotemporal functional connectivity in schizophrenia associated with auditory hallucinations. *Biol Psychiatry* 51:1008–1011.
- Lazarewicz MT, Ehrlichman RS, Maxwell CR, Gandal MJ, Finkel LH, Siegel SJ (2010) Ketamine modulates theta and gamma oscillations. *J Cogn Neurosci* 22:1452–1464.
- Lichtman AH, Dimen KR, Martin BR (1995) Systemic or intrahippocampal cannabinoid administration impairs spatial memory in rats. *Psychopharmacology* 119:282–290.
- Lisman J, Buzsáki G (2008) A neural coding scheme formed by the combined function of gamma and theta oscillations. *Schizophr Bull* 34:974–980.
- Melges FT, Tinklenberg JR, Hollister LE, Gillespie HK (1970) Marihuana and temporal disintegration. *Science* 168:1118–1120.
- Meyer-Lindenberg AS, Olsen RK, Kohn PD, Brown T, Egan MF, Weinberger DR, Berman KF (2005) Regionally specific disturbance of dorsolateral prefrontal-hippocampal functional connectivity in schizophrenia. *Arch Gen Psychiatry* 62:379–386.
- Morrison PD, Nottage J, Stone JM, Bhattacharyya S, Tunstall N, Brenneisen R, Holt D, Wilson D, Sumich A, McGuire P, Murray RM, Kapur S, Ffytche DH (2011) Disruption of frontal theta coherence by delta(9)-tetrahydrocannabinol is associated with positive psychotic symptoms. *Neuropsychopharmacology* 36:827–836.
- O'Keefe J, Recce ML (1993) Phase relationship between hippocampal place units and the EEG theta rhythm. *Hippocampus* 3:317–330.
- Pape HC, Narayanan RT, Smid J, Stork O, Seidenbecher T (2005) Theta activity in neurons and networks of the amygdala related to long-term fear memory. *Hippocampus* 15:874–880.
- Paxinos G, Watson C (2008) *The rat brain in stereotaxic coordinates*, Fourth Edition. New York: Academic.
- Puighermanal E, Marsicano G, Busquets-García A, Lutz B, Maldonado R, Ozaita A (2009) Cannabinoid modulation of hippocampal long-term memory is mediated by mTOR signaling. *Nat Neurosci* 12:1152–1158.
- Raghavachari S, Kahana MJ, Rizzuto DS, Caplan JB, Kirschen MP, Bourgeois B, Madsen JR, Lisman JE (2001) Gating of human theta oscillations by a working memory task. *J Neurosci* 21:3175–3183.
- Robbe D, Buzsáki G (2009) Alteration of theta timescale dynamics of hippocampal place cells by a cannabinoid is associated with memory impairment. *J Neurosci* 29:12597–12605.
- Robbe D, Montgomery SM, Thome A, Rueda-Orozco PE, McNaughton BL, Buzsáki G (2006) Cannabinoids reveal importance of spike timing coordination in hippocampal function. *Nat Neurosci* 9:1526–1533.
- Sauseng P, Griesmayr B, Freunberger R, Klimesch W (2010) Control mechanisms in working memory: a possible function of EEG theta oscillations. *Neurosci Biobehav Rev* 34:1015–1022.
- Siapas AG, Lubenov EV, Wilson MA (2005) Prefrontal phase locking to hippocampal theta oscillations. *Neuron* 46:141–151.
- Siegel M, Warden MR, Miller EK (2009) Phase-dependent neuronal coding of objects in short-term memory. *Proc Natl Acad Sci U S A* 106:21341–21346.
- Sigurdsson T, Stark KL, Karayiorgou M, Gogos JA, Gordon JA (2010) Impaired hippocampal-prefrontal synchrony in a genetic mouse model of schizophrenia. *Nature* 464:763–767.
- Solowij N, Michie PT (2007) Cannabis and cognitive dysfunction: parallels with endophenotypes of schizophrenia? *J Psychiatry Neurosci* 32:30–52.
- Tort AB, Kramer MA, Thorn C, Gibson DJ, Kubota Y, Graybiel AM, Kopell NJ (2008) Dynamic cross-frequency couplings of local field potential oscillations in rat striatum and hippocampus during performance of a T-maze task. *Proc Natl Acad Sci U S A* 105:20517–20522.
- Uhlhaas PJ, Singer W (2006) Neural synchrony in brain disorders: relevance for cognitive dysfunctions and pathophysiology. *Neuron* 52:155–168.
- Uhlhaas PJ, Singer W (2010) Abnormal neural oscillations and synchrony in schizophrenia. *Nat Rev Neurosci* 11:100–113.
- van der Meer MA, Redish AD (2011) Theta phase precession in rat ventral striatum links place and reward information. *J Neurosci* 31:2843–2854.
- Varela F, Lachaux JP, Rodriguez E, Martinerie J (2001) The brainweb: phase synchronization and large-scale integration. *Nat Rev Neurosci* 2:229–239.
- von Stein A, Sarnthein J (2000) Different frequencies for different scales of cortical integration: from local gamma to long range alpha/theta synchronization. *Int J Psychophysiol* 38:301–313.
- Wang GW, Cai JX (2006) Disconnection of the hippocampal-prefrontal cortical circuits impairs spatial working memory performance in rats. *Behav Brain Res* 175:329–336.
- Wise LE, Thorpe AJ, Lichtman AH (2009) Hippocampal CB1 receptors mediate the memory impairing effects of delta9-tetrahydrocannabinol. *Neuropsychopharmacology* 34:2072–2080.
- Yoon T, Okada J, Jung MW, Kim JJ (2008) Prefrontal cortex and hippocampus subserve different components of working memory in rats. *Learn Mem* 15:97–105.